engineering proceedings

MDPI

Proceedings Paper,

A High Precision Robotic System Design for Microsurgical Applications. †

Xiaoyu Huang[1], Elizabeth Rendon-Morales[1] and Rodrigo Aviles-Espinosa[1,*]

[1] Robotics and Mechatronics Systems Research Group, School of Engineering and Informatics, University of Sussex, UK; ra408@sussex.ac.uk
* Correspondence: ra408@sussex.ac.uk
† Presented at the 10th International Electronic Conference on Sensors and Applications (ECSA-10), 15–11 30 November 2023; Available online: https://ecsa-10.sciforum.net/.

Abstract: The introduction of robotic systems in medical surgery has achieved the goal of decreasing procedures invasiveness positively impacting the patient's prognosis by reducing the incisions size, surgical infections, and hospitalization time. Nowadays robotic surgery is used as an integral part of urology, gynecology, abdominal and cardiac interventions. Despite its adoption in several surgical specialties, robotic technology remains limited in the area of microsurgery. In this paper, we present the development of a robotic system providing sub-millimeter motion resolution for the potential manipulation of fine structures. The design is based on a linear delta robotic geometry. The motion, resolution and repeatability of the developed system were simulated followed by a proof-of-concept experimental testing. The developed system achieved a motion resolution of 3.37 ±0.17µm in both the X and Y axes and 1.32 ±0.2µm in the Z axis considering individual steps. We evaluated the system navigation setting a zigzag trajectory having dimensions below those found in blood vessels (300 to 800 µm) and found that the system is capable of achieving a maximum resolution of 3.06 ±0.03 µm. These results demonstrate the potential application of the here presented robotic system for its use in microsurgical applications such as neurosurgery, plastic, and breast cancer surgeries.

Keywords: robot design; parallel robot; microsurgery; high precision.

Citation: To be added by editorial staff during production.

Academic Editor: Firstname Lastname

Published: 15 November 2023

Copyright: © 2023 by the authors. Submitted for possible open access publication under the terms and conditions of the Creative Commons Attribution (CC BY) license (https://creativecommons.org/licenses/by/4.0/).

1. Introduction

Within the last two decades, multiple efforts have been focused on introducing robotic surgeries in routine procedures within multiple surgical disciplines [1] spanning from ophthalmology, urology gynecology, cardiology etc. The benefits of such technology compared to open surgery include the reduction of incisions from centimeters to tens of millimeters, resulting in minimized patient trauma, reduction in surgical site infections and shorter hospitalization time, providing benefits to the patient's recovery. Current commercial robotic systems allow the surgeon to manipulate the laparoscopic tools though a set of controls which translate the surgeon's natural hand and wrist movements into corresponding surgical tool movements providing millimetric precision required for general surgical procedures.

However specialized procedures requiring sub-millimeter precision manipulation such as reconstructive microsurgeries, surgical anastomosis, vitreoretinal eye surgery, and neurosurgery have not yet benefited from robotic surgery [2, 3], posing the need for the development of robotic systems specially designed for such applications. Surgical anastomosis is a surgical technique used to make a connection between tubular body structures such as blood vessels, having diameters ranging between 300 and 800µm. Reconnection of such structures is key to the re-establishment of lymphatic flow required in vascularized tissue transplantation [4]. Commercial platforms such as the da Vinci robot have been used to attempt procedures requiring high precision manipulation such as microsurgical anastomosis. However, the design specifications of such systems are best suited to perform key-hole surgeries that deal with structures having dimensions in the centimeters range [5], making challenging the provision of sufficient motion resolution to accomplish tasks at micro-scale level. State of the art examples of robotic systems capable of achieving high precision actuation are limited. These have been mainly evaluated in research laboratories trialing microsurgical applications including blood vessels nerve tracts and other soft tissue structure reconnection. Initial first in human surgeries reported in literature include lymph venous anastomosis required for breast cancer-related lymphedema treatment [6]. Here, the surgeon's movements can be downscaled down to ~70 um motion precisions well beyond key-hole surgical robots. Other robotic systems developed for microsurgical applications include the MUSA robot [7] and MMI's Symani System with NanoWrist (Italy) [8]. These systems provide magnification of the surgical area allowing simplified implementations in the operating room to perform micro-surgical procedures. Such robots are based on serial link geometries designed to cover larger workspaces. This, however, possesses the challenge of cumulative backlash errors which are often compensated using pre-loaded differential gears impacting on the robot complexity often associated with price [9].

In this paper, we present the design and simulation of a surgical robotic system based on a parallel geometry aiming to reduce the design complexity while providing sub-millimeter motion resolution. Using this type of geometry, the robot link dimensions were tailored for having a defined workspace and resolution suited for microsurgical tasks. The motion, resolution and repeatability of the developed system were assessed though simulations followed by an experimental proof-of-concept high precision mimicking a stitching task to validate its potential to be used for microsurgical procedures.

2. Materials and methods

In a parallel robot geometry, the end-effector is connected to the base multiple link sequences, forming a closed-loop system. This has been widely used in industrial pick and place applications [8]. The iimplementation of parallel structures can be used to simplify the robot design while achieving high precisions [9].

The design of the proposed surgical robotic system is based on a linear delta robotic geometry consisting of three linear actuators, three pairs of parallel legs and twelve spherical joints, enabling high stability, low inertia, and high motion precision all required for microsurgical tasks. Thus, in this paper we describe the robot design methodology consisting of three stages: geometrical structure design, robot simulation, validation, and robot proof-of-concept testing.

2.1. Geometrical structure design

The simplified geometrical model of the linear delta robot design is shown in Fig. 1.

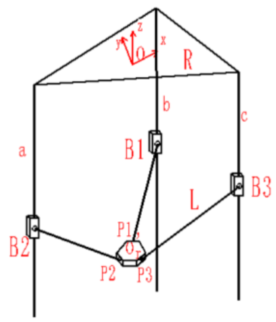

Figure 1. Geometrical construction of linear delta robot.

Here, the ball joints are fixed to linear sliders (B1, B2, B3) and the end-effector (P1, P2, P3). The coordinate of the base plane O is (0, 0, 0), the coordinate of the end-effector O′ (x, y, z), and the displacement of the linear sliders are z1, z2, z3, respectively. This implies that the coordinates of the B1, B2, B3 are (0, √3/2, z1), (-√3/2, z2), (√3/2, 0, z3) respectively. The geometrical relationship between arm length L, the radius of the based platform R, and the radius of the move platform are obtained, using equations (1)-(4).

Equation 1 shows the spatial relationship between robotic arms and the center of the mobile platform using vector arithmetic, to express the arm length L.

Equations 2-4 are related by the robotic arm length L which is obtained by end-effector coordinates (x, y, z), r, R, and the vertical motion of the 3 linear sliders z1, z2, and z3 respectively. Through mathematical simplifications the equations of x, y, z or z1, z2, z3 can be obtained.

$$\overrightarrow{OO'} = \overrightarrow{OBi} + \overrightarrow{BiPi} + \overrightarrow{PiO'} \tag{1}$$

$$x^2 + (y + r - R)^2 + (z - z1)^2 = L^2 \tag{2}$$

$$\left(x - \frac{\sqrt{3}}{2}(r - R)\right)^2 + \left(y - \frac{1}{2}(r - R)\right)^2 + (z - z2)^2 = L^2 \tag{3}$$

$$\left(x - \frac{\sqrt{3}}{2}(r - R)\right)^2 + \left(y - \frac{1}{2}(R - r)\right)^2 + (z - z3)^2 = L^2 \tag{4}$$

2.2. Kinematic simulation

Using equations (1) to (4) while defining the motion limits of B1, B2 and B3, the motion state of the end-effector O′ was represented dynamically through simulations. The robot design and the kinematics modeling were simulated using MATLAB 2020 (Math Works, USA) and CATIA V5-6R2018 (Dassault systems, France).

Following the geometric solution of forward kinematic, simulation results showed that the motion resolution considering the final arm length and the base platform radius (L= 250mm, R=235mm, r=20mm) ranges between 0.24-0.625µm. Thus, the minimum single-step motion resolution of a single motor is 0.625µm considering micro-stepping of 1/8. Figure 2 presents an example trace resulting from the simulations outlining the temporal evolution of the XY*Z*-axis coordinates of the end-effector. Figure 2a shows the displacement of the *X*-axis and *Y*-axis coordinates over time, and Figure 2b shows the *Z*-axis coordinate displacement over time. From these results, it can be observed that the maximum achieved motion resolution under the final dimension parameters is ~ 0.24 µm.

To assess the robotic workspace considering the obtained dimensions (L, R, and r) all simulated trajectory points of the end-effector O' were traced. Figure 2c shows the front view of the simulated full workspace having a pyramid like structure with dimensions of ~114.2 mm x 114.2 mm x 110 mm and 130mm depth.

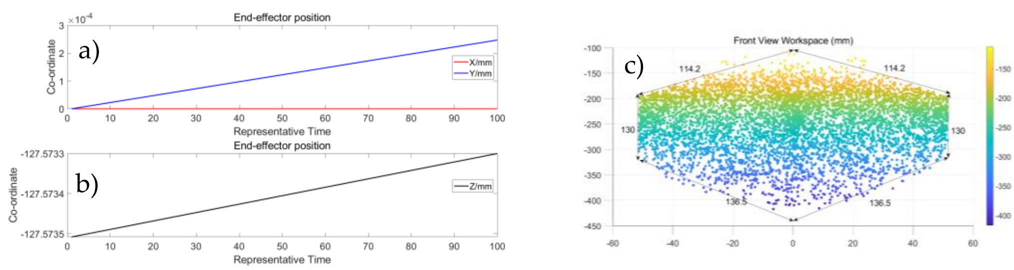

Figure 2. Temporal evolution of the XY*Z*-axis coordinates of the end-effector, (a) coordinates changes in X and Y axis (b) temporal resolution of Z axis. (c) Front view of the workspace obtained through simulations.

The forward kinematic simulation shows that the end-effector resolution of the linear delta robot can reach a maximum of 0.36μm/pulse considering 1/8 micro-stepping and 1.75μm/pulse considering 1/2 micro-stepping. By integrating both the workspace and motion resolution it can be concluded that using the design parameters obtained (R = 250mm, L=235mm, r=20mm), it is possible to reach the required precision for microsurgical applications dealing with structures having dimensions between 300 to 800 μm [10].

The inverse kinematic (IK) simulation was used to determine the accuracy of the stepper actuators setting and to guarantee, through simulations, that the system configuration will match the sub-millimeter level performance required for microsurgical applications. The IK expressions are represented in a similar fashion to the forward kinematics. Here the positions B1, B2 and B3 were expressed as the positions of end-effector (x, y, z). Following the geometrical construction of the linear delta robot shown in Figure 1, the coordinates of the linear sliders on the XY plane were considered to be fixed, then the change of the coordinates is reflected in the displacement of the *z*-axis coordinates relative to the initial position (z1, z2, z3). The real-time *z*-axis coordinates of B1, B2 and B3 can be obtained through equations (5)-(7):

$$z1 = \pm\sqrt{L^2 - x^2 - (y + r - R)^2} + z \tag{5}$$

$$z2 = \pm\sqrt{L^2 - \left(x - \frac{\sqrt{3}}{2}(r - R)\right)^2 - \left(y - \frac{r - R}{2}\right)^2} + z \tag{6}$$

$$z3 = \pm\sqrt{L^2 - \left(x - \frac{\sqrt{3}}{2}(R - r)\right)^2 - \left(y - \frac{r - R}{2}\right)^2} + z \tag{7}$$

Note that equations (5)-(7) show the vertical motion of the linear sliders z1, z2, z3 expressed by the parameters L, R, r, which are affected by end-effector's position (x, y, z). The notation ± corresponds to the robotic motion direction where a positive sign indicates a downwards movement of the end-effector's position.

Figure 4 shows the IK simulation results of a zigzag trajectory. Figure 4a) shows the zigzag trajectory in the XY plane consisting of horizontal and vertical displacements set to describe 150μm and 15μm segments, respectively. Fig 4b shows the coordinate changes of the end-effector in the XY plane while figure 4c shows the changes of three robot sliders (Z1, Z2, Z3). In this case, a 15μm-150μm displacement of the end-effector, produces a displacement of 25.4μm-218.7μm the three linear sliders of the robot.

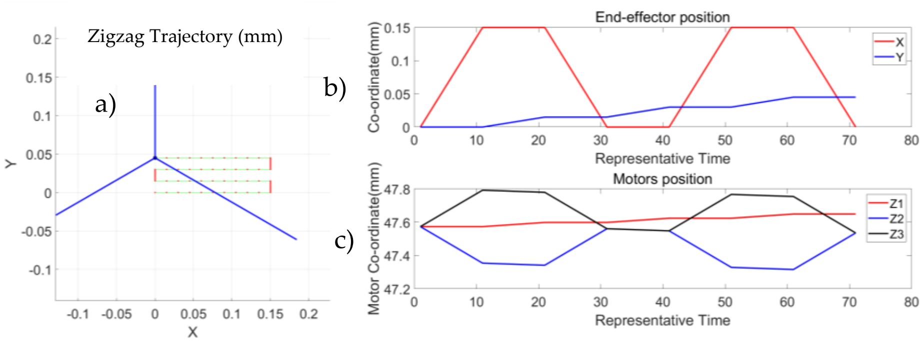

Figure 4. Zigzag trajectory tracking results of IK simulation.

3. Results and discussion

3.1. Robot proof-of-concept trayectiry testing

Considering the geometric design and simulation results described in Section 2, the proposed robotic system was built employing metallic beams (MakerBeam B.V., Netherlands), and custom-made 3D printed components. Figure 5a shows the physical prototype (top view) of robotic platform. The drive system uses three 35mm SH3533-12U40 stepper motors (Sanyo Denki, Japan) and a BSD 02.V motor driver (RTA Pavia, Italy). The robotic system is controlled though a custom-made GUI controlled by MyRIO 1900 FPGA (NI, USA).

For the evaluation of the precision and kinematic performance of the linear delta robot manipulator, a noncontact metrology approach based on bright field microscopy system was used. To reach the required micron level resolution, the linear sliders displacement was set to 20 micron/pulse, corresponding to an angular movement of 0.225°. This resulted in a motion resolution of 1.32 ±0.02μm for the z axis and 3.37 ±0.17μm for the X and Y axes indicating the system's potential to be used for microsurgical tasks [11]. The motion performance of the proposed robotic system was set up in a laboratory environment and evaluated though a proof-of-concept experimental evaluation shown in figure 5. We define a zigzag/raster trajectory which consisted of 5-stage 180μm horizontal lines and 4-stage 15μm vertical lines. For each test, three forward trajectories and three backward trajectories were operated.

The representative zigzag trajectory test was set up in the LabVIEW software considering the dimensions of fine structures such as skin cells having an average size of 50 μm [11]. For data analysis videos of the executed trajectory were recorded. By tracing a zigzag 2D trajectory, we aim at simulating a simplified stitching procedure where the end-effector is to be moved from side to side to join adjacent portions of tissue. The zigzag 2D trajectory is shown in Figure 5. Figure 5b is the executed zigzag trajectory without compensation as it can be observed the resulted in differences between trajectory segments and figure. This is to be expected as the robot operates in an open loop configuration.

However, further analysis of the traces indicated repeatable offset errors within the trajectory which can be further compensated. The results after trajectory compensation are presented in figure 5c. Table 1 shows the detailed results of the compensated zigzag trajectory. It can be observed that the average trajectory error is improved from 40 ±2.13 μm (uncompensated trajectory) to 5.64 ±0.63 μm (compensated trajectory) with an average angular error reduction of 2.7 ±0.54°. Assessing the resolution obtained within this proof-of-concept test resulted in an average motion resolution of 3.06 ±0.03 μm.

Comparing the results obtained from the simulations and experiments, it can be concluded that the built system dynamics, and the open loop control affect the obtained motion accuracy. This is expected as the built system elements specifications and tolerances differ for the ideal conditions set in the simulations. None the less, the motion resolution was found to be less than 5 microns, indicating that the system offers a performance that goes well beyond that required for performing microsurgical operations.

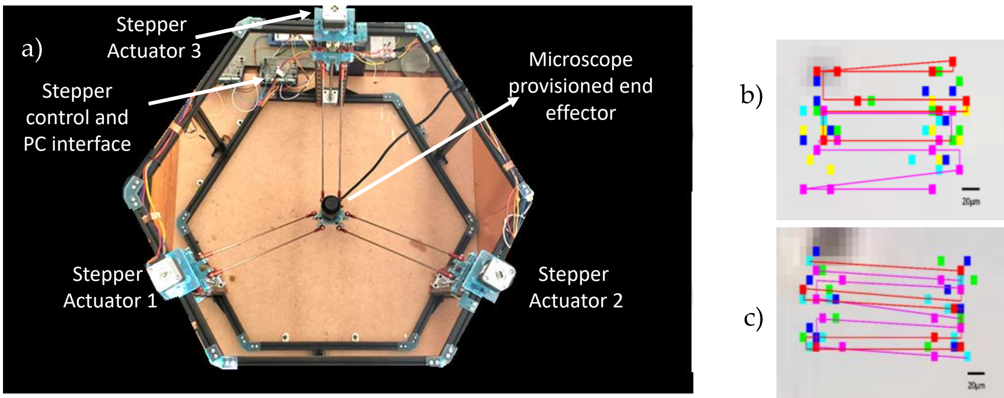

Figure 5. (a) Physical prototype of the developed robotic platform (top view), (b) zigzag trajectory without compensation and (c) with compensation

Table 1. Test results of the compensated zigzag trajectory.

No.	Resolution[μm]	Angle error [°]	Trajectory error[μm]
Zigzag 1	3.17±0.03	-2.52±0.85	9.59±0.91
Zigzag 2	3.08±0.04	-2.30±0.25	3.47±0.65
Zigzag 3	2.94±0.02	-3.28±0.53	3.85±0.34
Average	3.06±0.03	2.7±0.54	5.64±0.63

4. Conclusion

In this paper, the design, simulation, and proof-of-concept evaluation of a linear delta robot device to be used for microsurgical applications has been presented. The robot design was focused on achieving high motion precision tasks considering the dimensions of structures such as blood vessels ranging between 300 to 800 μm.

This resulted in a system having dimensions of R = 250mm, L=235mm, r=20mm and a pyramid like workspace with dimensions of ~114.2 mm x 114.2 mm x 110 mm and 130 mm depth. This resulted in a motion resolution of 3.37 ±0.17μm in both the X and Y axes and 1.32 ±0.2μm in the Z axis considering individual steps. The system was evaluated considering a zigzag trajectory with dimensions similar to those found in blood vessels. We found that performing the zigzag trajectory in a series of three experiments resulted in a displacement between these resulting in an error of 40 ±2.13μm. Though the addition of displacement and angle compensation these errors were reduced by 85.9%. These results demonstrate the potential application of the here presented robotic system for its use in microsurgical procedures.

Acknowledgments: Xiaoyu Huang acknowledges the University of Sussex scholarship for his PhD studies. The authors acknowledge the in-kind contributions from EAO LTD.

References

1. Morrell, A.L.G., A.C. Morrell-Junior, A.G. Morrell, J.M.F. Mendes, F. Tustumi, D. E-Oliveira-E-Silva LG, and A. Morrell. "The History of Robotic Surgery and Its Evolution: When Illusion Becomes Reality." Rev Col Bras Cir 48 (2021): e20202798.
2. Diana, M., and J. Marescaux. "Robotic Surgery." Br J Surg 102, no. 2 (2015): e15-28.
3. Bhandari, M., T. Zeffiro, and M. Reddiboina. "Artificial Intelligence and Robotic Surgery: Current Perspective and Future Directions." Curr Opin Urol 30, no. 1 (2020): 48-54.
4. Brodie, A., and N. Vasdev. "The Future of Robotic Surgery." Ann R Coll Surg Engl 100, no. Suppl 7 (2018): 4-13.
5. Lai, C.S., C.T. Lu, S.A. Liu, Y.C. Tsai, Y.W. Chen, and I. C. Chen. "Robot-Assisted Microvascular Anastomosis in Head and Neck Free Flap Reconstruction: Preliminary Experiences and Results." Microsurgery 39, no. 8 (2019): 715-20.
6. van Mulken, T.J.M., R.M. Schols, A.M.J. Scharmga, B. Winkens, R. Cau, F.B.F. Schoenmakers, S.S. Qiu, Rrwj van der Hulst, and Group MicroSurgical Robot Research. "First-in-Human Robotic Supermicrosurgery Using a Dedicated Microsurgical Robot for Treating Breast Cancer-Related Lymphedema: A Randomized Pilot Trial." Nat Commun 11, no. 1 (2020): 757.
7. Yang, U.J., D. Kim, M. Hwang, D. Kong, J. Kim, Y.H. Nho, W. Lee, and D. S. Kwon. "A Novel Microsurgery Robot Mechanism with Mechanical Motion Scalability for Intraocular and Reconstructive Surgery." Int J Med Robot 17, no. 3 (2021): e2240.
8. Savastano, A., and S. Rizzo. "A Novel Microsurgical Robot: Preliminary Feasibility Test in Ophthalmic Field." Transl Vis Sci Technol 11, no. 8 (2022): 13.
9. Aitzetmuller, M.M., M.L. Klietz, A.F. Dermietzel, T. Hirsch, and M. Kuckelhaus. "Robotic-Assisted Microsurgery and Its Future in Plastic Surgery." J Clin Med 11, no. 12 (2022).
10. Pusca, A., R. Gabriela, I. Birlescu, C. Vaida, A. Pisla, C. Schonstein, B. Gherman, P. Tucan, and D. Pisla. "Workspace Analysis of Two Innovative Parallel Robots for Single Incision Laparoscopic Surgery." Acta Technica Napocensis-Series: Applied Mathematics, Mechanics, and Engineering 65 (2022): 25.
11. Huang, X.Y., E. Rendon-Morales, and R. Aviles-Espinosa. "Towards Cellular Level Microsurgery: Design and Testing of a High Precision Delta Robot for Medical Applications." In Hamlyn Symposium on Medical Robotics 2023. Royal Geographical Society, 2023.

Disclaimer/Publisher's Note: The statements, opinions and data contained in all publications are solely those of the individual author(s) and contributor(s) and not of MDPI and/or the editor(s). MDPI and/or the editor(s) disclaim responsibility for any injury to people or property resulting from any ideas, methods, instructions, or products referred to in the content.